sensors

MDPI

Article

Comparison of Amplitude Measurements on Borehole Geophone and DAS Data

Sana Zulic, Evgenii Sidenko, Alexey Yurikov, Konstantin Tertyshnikov, Andrej Bona and Roman Pevzner *

Centre for Exploration Geophysics, Curtin University, Bentley, WA 6151, Australia
* Correspondence: r.pevzner@curtin.edu.au

Abstract: DAS and geophones are the two most popular sensors for borehole seismic acquisition. As such, it is important to get a good understanding of how these two types of sensors compare to each other. The natural measurand for the techniques is different; millivolts are approximately proportional to particle velocities for geophones vs. changes in the phase of light linked to the changes in strain on the sensing fibre. This paper focuses on the experimental comparison of absolute values of these measurands derived from a VSP survey acquired in Curtin GeoLab training well. We describe the acquisition setup for the walk-away VSP acquired with DAS and geophones, allowing the direct comparison and the workflow, which we can use to represent the data in strain rate. Albeit this is unlikely to be universal, we find that the absolute values are similar for this experimental setup.

Keywords: borehole seismic; geophones; DAS; innovative technologies

check for updates

Citation: Zulic, S.; Sidenko, E.; Yurikov, A.; Tertyshnikov, K.; Bona, A.; Pevzner, R. Comparison of Amplitude Measurements on Borehole Geophone and DAS Data. *Sensors* **2022**, *22*, 9510. https://doi.org/10.3390/s22239510

Academic Editor: Yih-Min Wu

Received: 8 November 2022
Accepted: 2 December 2022
Published: 5 December 2022

Publisher's Note: MDPI stays neutral with regard to jurisdictional claims in published maps and institutional affiliations.

Copyright: © 2022 by the authors. Licensee MDPI, Basel, Switzerland. This article is an open access article distributed under the terms and conditions of the Creative Commons Attribution (CC BY) license (https://creativecommons.org/licenses/by/4.0/).

1. Introduction

The rapid uptake of distributed acoustic sensing (DAS) for borehole seismic acquisition prompts fundamental research to identify how its performance compares to the performance of conventional borehole geophone sensors. These two types of sensors, DAS and geophones, are fundamentally different. The geophones are electro-mechanical sensors that sense the motion of the earth in the form of particle velocity. In contrast, DAS observes a change in elongation of an optical fibre that acts as the sensor. The geophone consists of a permanent magnet mounted on a spring with a conductor (copper wire or coil) around it. When the earth moves, the magnet and coil also move. This movement generates a voltage across the coil's winding, which is proportional to the rate at which the coil cuts the magnetic flux, that is, to the velocity of the earth's motion [1]. In the case of borehole geophone, the geophone is mounted inside a downhole probe's housing, suspended in the borehole by an armoured cable and clamped to the formation at each desired depth. DAS utilises a fibre-optic (FO) cable, along which the interrogator unit (IU) emits a light pulse and registers how the phase of the backscattered light changes over time in sampling points [2]. The change in phase of backscattered light is proportional to the fibre deformation caused by the earth's motion. Although there is no standard for a DAS system in terms of its generic architecture, in summary, DAS measurements are said to be proportional to the average strain or strain rate between two sampling points separated by a gauge length.

For borehole seismic measurements, a fibre-optic sensing cable is deployed in the well. Borehole geophones and DAS have different factors that affect the measured signal. For example, the geophone measurements are affected by the geophone type and its performance, the probe's housing, the quality of the probe's coupling to the formation or the casing, etc. [3,4]. The DAS measurements are affected by the cable design, the cable's coupling to the formation, optical parameters, the interrogator design, etc. [2,5–7]. Therefore, it is reasonable to question whether these systems can obtain the same information about the same physical properties. Wang, et al. [8] demonstrated on real and synthetic data that amplitudes of the strain waveforms computed from geophone waveforms are comparable to those obtained by DAS.

Initial DAS tests for borehole seismic application used preinstalled cables behind the casing or on tubing inside the casing and demonstrated that seismic energy could be detected on FO cable at a depth over 4 km [9–11]. Daley, et al. [12] showed a variety of DAS deployment and acquisition possibilities, in which data quality varied significantly depending on these. Mateeva, et al. [5] qualitatively compared geophone to DAS and concluded that DAS polarity is independent of the wave propagation direction and that while transmitted waves have the same polarity as on the geophone dataset, the reflected DAS waves have opposite polarity to reflections on the geophone dataset. Dean, et al. [13] attempt to clarify the nature of DAS measurements, and on examples from synthetic and real data, they show their DAS system measure instantaneous strain and that the time derivative of strain (the strain rate) is proportional to the average velocity measured at all points along the gauge length. In addition to this, they showed that DAS has highly complex directionality that is dependable on wavenumber and angle of incidence. Correa, et al. [6] compared seismic data obtained by DAS and conventional borehole seismic sensors to understand DAS data more and showed that DAS could provide similar or better data quality. As DAS measures strain or strain rate, and geophone measures particle velocity, several methods could be used to convert one property to the other. Most of the published literature is related to the conversion of DAS data to particle velocity, where it is either necessary to rescale the time-integrated DAS data [14] or apply a conversion filter [15] which accounts for pulse and gauge length. The former requires the knowledge of local propagation velocity, while the latter needs to be regularised by adding the noise to DAS data to avoid division by zero that may occur for certain wavenumbers. However, Isaenkov, et al. [16] had difficulties applying the filter for larger wavenumber and suggested that internal interrogator processing may contribute to DAS response deviating from a strain rate.

Moreover, various DAS interrogators can have very different designs. The differences in the design of DAS recording units and selection of acquisition parameters significantly affect the data quality [2,13,17,18]. Therefore, further research on DAS is required to better identify the strengths and limitations of DAS technology and assess how DAS measurements correspond to standard borehole geophone recordings.

These tasks are best accomplished in a controlled environment at designated test sites that should allow for the repetition of the experiment using different sensors in stable conditions. In addition, such test sites should enable the comparison of different seismic receivers for both borehole and surface arrays using different types of seismic sources. There are several test facilities for carbon capture and storage (CCS) around the globe, where DAS technology is used, including CaMI [19], Otway International Test Centre [20], CSIRO In-Situ Laboratory [21] and RITE [22]. However, access to the data from these project-based sites is often restricted and not publicly available. Furthermore, this type of testing is not limited to these CCS sites; standard telecommunication fibre-optic (FO) cables as seismic DAS sensors were compared to conventional seismometers by Lindsey, et al. [23], Lindsey, et al. [24] and Ajo-Franklin, et al. [25]. Lastly, the fundamental research on DAS is conducted at specifically developed test sites for trialling DAS technology: Aramco Houston Research Centre built for testing borehole arrays [26]; NOR-FROST [27] used to study the performance of surface DAS arrays and their coupling in different mediums; and the GeoLab Research facility at Curtin University, where DAS response can be studied from both surface and borehole DAS array, and compared to the reference geophone datasets.

In this paper, we compare DAS and geophone data acquired during the walkway vertical seismic profile (VSP) experiment performed at the Curtin GeoLab in 2020. First, we convert the particle velocity data from the geophone dataset to the strain rate. Then we use the first-break amplitudes and the entire wavefield to compare the absolute values of the strain rate of both types of sensors. We demonstrate that the DAS response is similar to the geophone response converted to the strain rate averaged over the gauge length of the DAS system. Furthermore, we show that the amplitudes of the strain rate measured with DAS have similar absolute values to strain-rate amplitudes obtained using converted geophone

measurements—the losses of seismic energy due to the geophone coupling and housing are similar to the losses in the fibre-optic cable construction and installation.

2. Test Site: Curtin GeoLab Research Facility

The Curtin GeoLab Research Facility was established at Curtin University, Western Australia, with aims to conduct applied geophysical research, equipment testing and training of students and industry personnel. The key components of the GeoLab are a 900 m vertical well drilled on Curtin campus and state-of-the-art seismic equipment, which includes surface and borehole three-component geophones, impulse and vibroseis seismic sources and a variety of fibre-optic cables (including a cable permanently deployed in the borehole).

The Geolab Well (NGLd), previously referenced as the NGL training well [28], is located in the eastern onshore margin of Perth Basin (Figure 1). It comprises Quaternary (Q), Tertiary (T), Cretaceous (K) and Jurassic (J) aged sediments (Figure 2). The well is cased with fibreglass slotted between 650 and 890 m depth. A fibre-optic cable is cemented behind the casing with the loop at the bottom. The cable contains two single-mode fibres for distributed acoustic sensing and two multimode fibres for distributed temperature sensing. Since the entire length of the well is covered with fibre cores four times, this facility allows multiple FO interrogators to be used simultaneously [17]. It is also possible to deploy FO cables directly into the well to test the performance of different types of cables and the effect of the coupling on the measurements.

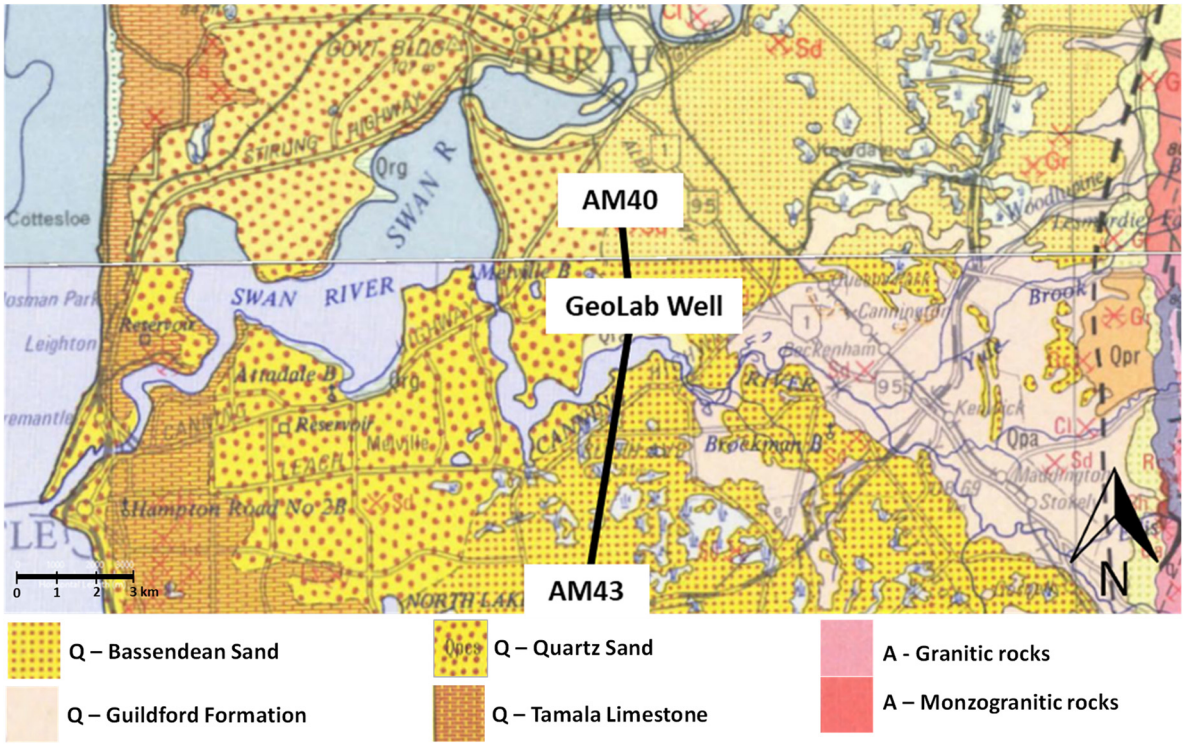

Figure 1. Geological map of the area around GeoLab Well-01 (© State of Western Australia (Department of Mines, Industry Regulation and Safety, 2020).

The GeoLab facility was previously used for a wide range of geophysical experiments: some were dedicated to comparing different borehole seismic receivers [28], and other experiments utilised different interrogator units and studied their internal characteristics and performance of various cable designs [18]. Shulakova, et al. [29] examined the use of the GeoLab well for passive registration of earthquakes and technogenic activities using DAS.

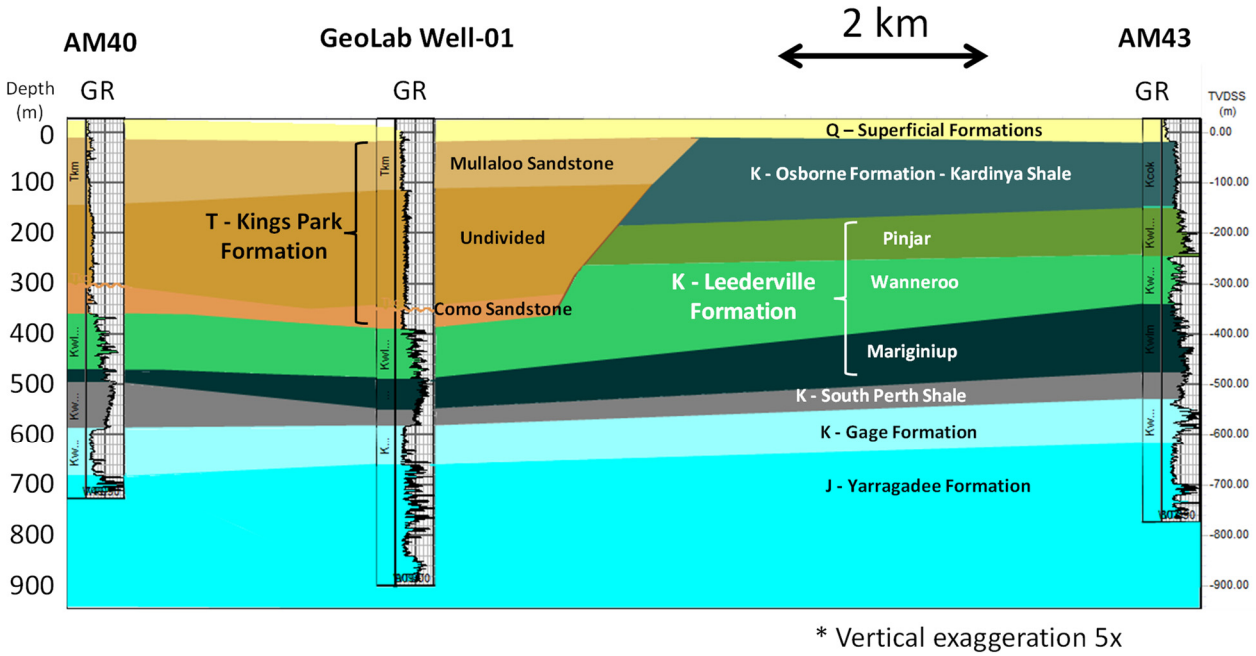

Figure 2. Geological cross-section along with three selected wells: AM40, GeoLab Well-01 and AM43.

This study uses data acquired during the walk-away VSP experiment carried out at the GeoLab in June 2020. The survey area with all source locations is shown in Figure 3. Aerial map showing the surface location of the well (blue) and source positions (red); every fifth source station is labelled. The data were acquired with a conventional three-component borehole geophone and a single-mode straight FO cable cemented behind the casing of the GeoLab Well-01. The seismic signal was generated by a 26,000 lb UniVib vibroseis truck. Acquisition parameters are given in Table 1.

Table 1. Seismic acquisition parameters.

VSP Survey Information	
Geophone Recording System	WaveLab II
Software acquisition	WaveControl
Logging cable	2500 m 4 conductor cable + electric winch
Geophone Information	
Downhole tool	Sercel 3C SlimWave with ten downhole shuttles Sensor: Omni 2400 15 Hz
Receiver step	10 m
Sweep + listen time	24 s + 4 s
Sample rate	1 ms
Sweep per receiver	1
DAS Information	
Interrogator unit	Silixa iDAS v2
Fibre-optic cable	Single-mode straight loose tube cable
Sampling interval raw/binned	1 m/5 m
Pulse length	5 m
Gauge length	10 m
Pulse Repetition Frequency	16 kHz (downsampled to 1 kHz)

Table 1. *Cont.*

Sample rate	1 ms (decimated to 2 ms for analysis)
Sweep per receiver	9
Source Information	
Source type	26,000 lb UniVib
Source sweep	8–150 Hz linear sweep
Sweep duration	24 s
Tapers	0.5 s
Force	70%
Source control	Pelton VibPro
Number of source locations	48

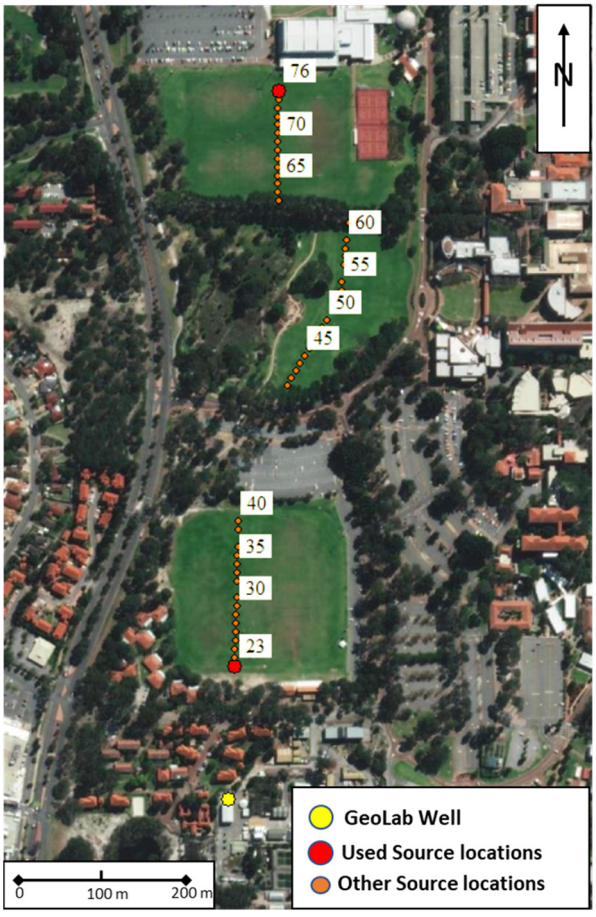

Figure 3. Aerial map showing the surface location of the well (blue) and source positions (red); every fifth source station is labelled.

3. Method

Direct comparison of geophone and DAS performance requires converting the data to the same physical property. In practice, DAS response is often converted to the particle velocity for comparison with geophone data [6,14]. Bakku [30] indicated that when we assume that DAS measures the strain rate, then it is given by the difference in the particle velocities measured by two vertical component geophones separated by a gauge length L:

$$\dot{\varepsilon}_{zz}^{DAS} = \frac{v_z\left(z + \frac{L}{2}\right) - v_z\left(z - \frac{L}{2}\right)}{L}, \quad (1)$$

where $\dot{\varepsilon}_{zz}^{DAS}$ is the strain rate along the vertical direction measured by a DAS system, v_z is the vertical component of particle velocity and z is the depth. We use this approach to convert the vertical component of particle velocity to the vertical component of strain rate.

We apply the following processing flow to get an absolute strain rate from the geophone dataset (summarised in Table 2). After loading raw geophone data, we apply descaling and geophone factors to calibrate the native system units (mV) to particle velocity (m/s). The conversion is based on acquisition parameters such as sampling rate, acquisition gain and the geophone type. The respective factors are obtained from the manufacturer's manual. Then we differentiate data over the 10 m interval (same interval as the gauge length used during acquisition of the DAS data) and assign the field geometry. The output dataset represents the strain rate (nanostrain/s), and we refer to it as converted geophone data. DAS native measurements are the phase variation of the laser light over time. Its native measurand is radians per second and is calibrated to the absolute strain rate (nanostrain/s) based on the acquisition settings of the gauge length, laser light wavelength and sampling frequency. The corresponding descaling factor provided by the manufacturer was applied. Then the geometry is assigned.

Table 2. Processing workflow for getting the absolute strain rate from geophone and DAS measurements.

Step	Converted Geophone	DAS
1	Read raw SEG-Y	Read relative strain-rate iDAS data
2	Apply descaling factor to get the voltage in millivolts	Apply descaling factor to get absolute strain rate
3	Apply geophone factor to get particle displacement rate in m/s	Assigning geometry
4	Assigning geometry	
5	Differentiate over the GL interval	

We firstly visually compare gathers from geophone, DAS and converted geophone datasets. Then we compare the amplitude spectrum of the entire absolute strain-rate wavefield (uncorrelated) and the first-break amplitudes (correlated) for DAS and converted geophone.

The gauge length is one of the most important DAS parameters as it affects both the resolution and signal-to-noise ratio of the acoustic signal [13]. The IU used in this survey has a fixed gauge length, and therefore, it was not possible to study the effect of the gauge length change. The proposed conversion allows adjustment of the gauge length. We can simulate different gauge lengths by differentiating the geophone data over different depth intervals. This simulation can assist with understanding this parameter and potentially use it for the sensitivity optimisation for a target wavelength. In addition to amplitude spectrum analysis and differentiation over a 10 m interval, we simulate the DAS response with two additional gauge lengths of 50 m and 90 m.

4. Data Analysis

To compare the performance of the DAS system and geophones, we use data from two source locations at the near offset (source location 23, 160 m) and the far offset (source location 76, 845 m).

Figures 4 and 5 show the comparison of the correlated vertical component geophone, DAS and converted geophone datasets for near and far offset, respectively. The geophone data have noisy channels because of the malfunctioning of two geophones in the receiver string (green arrows in Figure 5a), which is more prominent in the far offset data as the amplitude of the signal decays. This type of noise is consequently carried through to the converted geophone dataset. Apart from that, DAS and converted geophone records look similar, as shown in the selected trace view displayed at the bottom of the figures. The red

arrows indicate the difference in phase of P- and S direct waves between recorded DAS and converted geophone data.

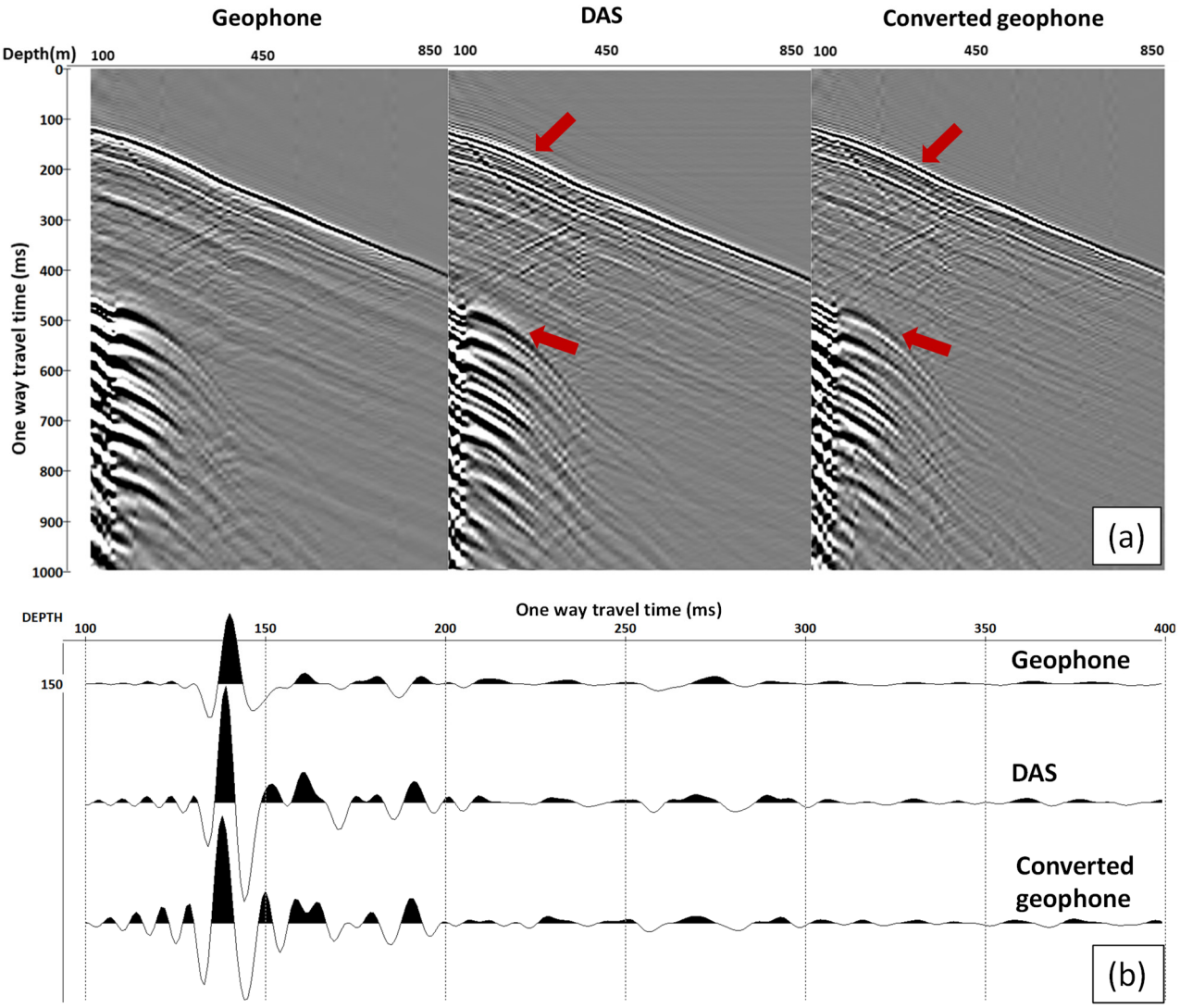

Figure 4. Near-offset example: (**a**) from left to right: gathers of geophone, DAS and converted geophone response; (**b**) from top to bottom: trace at a depth of 150 m of geophone, DAS and converted geophone response. We exclude every second trace from DAS data to match the same receiver interval for geophone/converted Geophone and DAS. The red arrows indicate the difference in phase of P- and S direct waves between recorded DAS and converted geophone data.

To compare the absolute values of the strain rate obtained using both types of sensors we analysed the uncorrelated wavefield. First, we applied Ormsby bandpass filter 5–8–150–200 Hz to denoise the data and adjusted the length of uncorrelated datasets to 27 s. Then we computed the average amplitude spectrum of the entire seismogram. Figure 6 shows the amplitude spectrum for near (a) and far (b) offsets for both types of receivers.

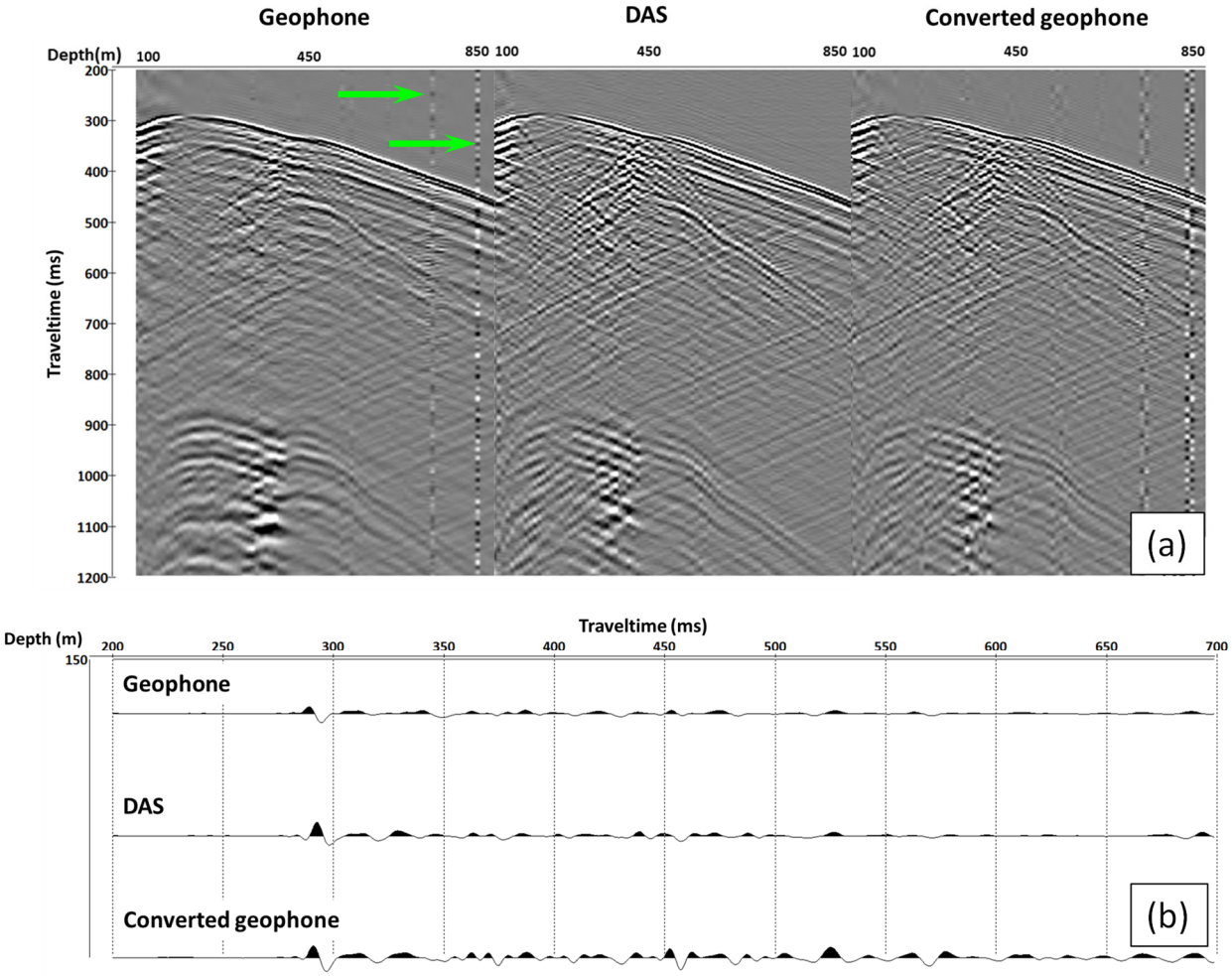

Figure 5. Far offset example: (**a**) gathers of geophone, DAS and converted geophone response; (**b**) trace at a depth of 150 m of geophone, DAS and converted geophone response. We exclude every second trace from DAS data to match the same receiver interval for geophone/converted geophone and DAS. The green arrows indicate locations of malfunctioning geophones.

The frequency spectrum of DAS and converted geophone data are similar for the near-offset shot. However, we observe more discrepancy in the spectrum with increased offset. The low-frequency signal of the DAS data has a lower amplitude compared to the converted geophone data, and towards the high frequency, the entire spectrum is biased (Figure 6b). Discrepancies for far offset data are most likely to be attributed to different directional sensitivity of DAS and geophones as at such offsets, seismic waves approach the vertical well at quite large angles. The prominent spikes/notches on the far offset spectra are the results of the interference of the multiples.

Then we correlate the data with the pilot sweep and compare the first-break amplitudes for near and far offsets (Figure 7a,b, respectively).

In addition to amplitude spectrum analysis, we simulate the DAS response with two additional gauge lengths by differentiation of geophone data over different depth intervals. The examples of converted geophone datasets obtained by differentiation over three simulated gauge lengths are shown in Figure 8, where the simulated gauge lengths are 10 m, 50 m and 90 m, from left to right.

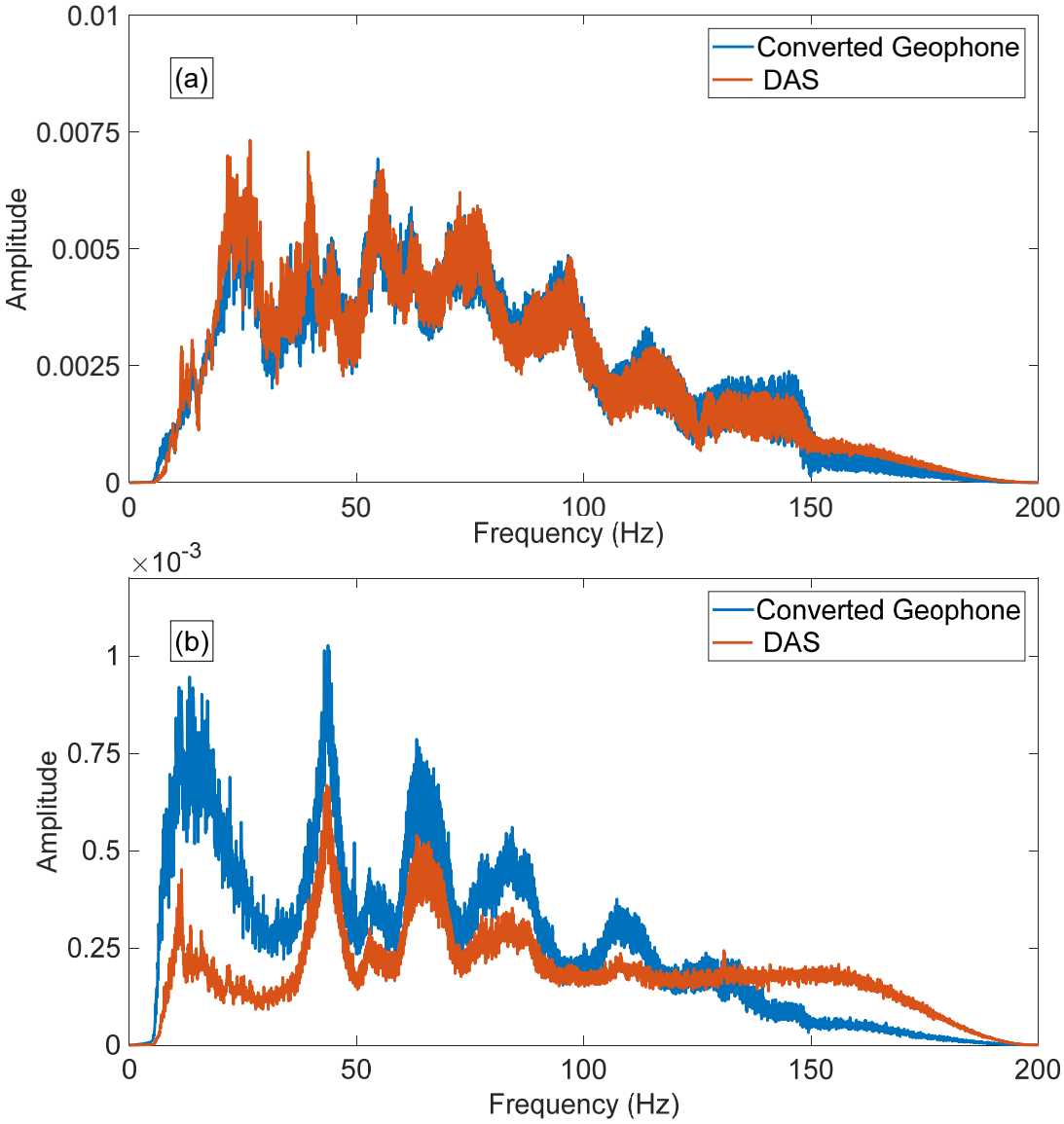

Figure 6. Amplitude spectrum comparisons for near (**a**) and far (**b**) offsets. The blue line is the strain rate from converted geophone, and the red line is the strain rate from DAS.

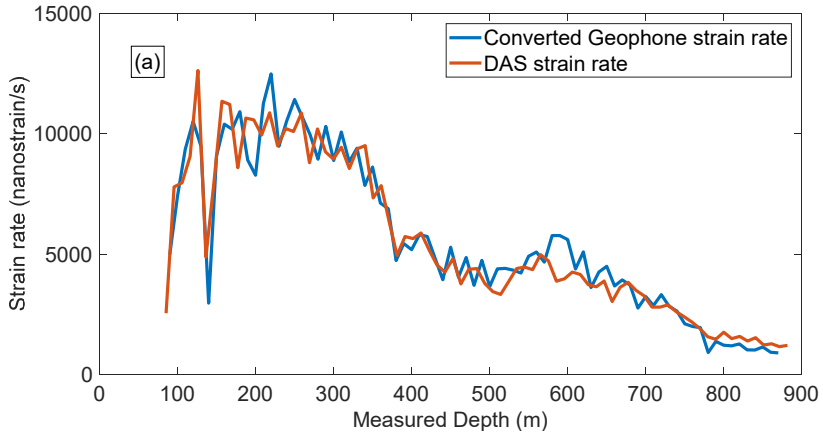

Figure 7. *Cont.*

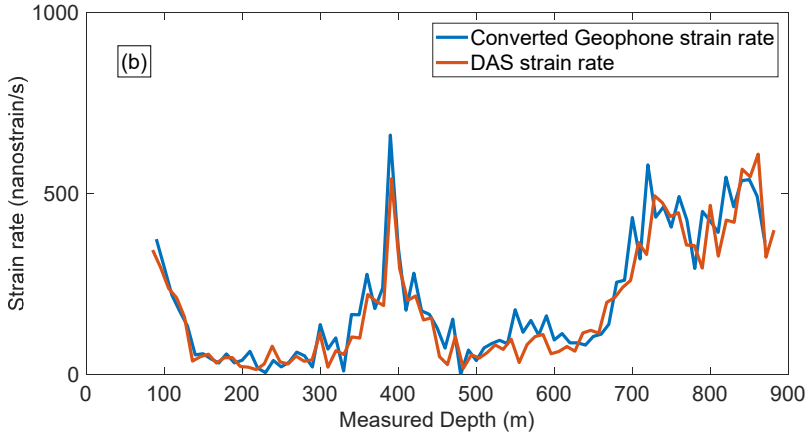

Figure 7. First-break amplitude comparison for near (**a**) and far (**b**) offset. The blue line is the strain rate from converted geophone, and the red line is the strain rate from DAS.

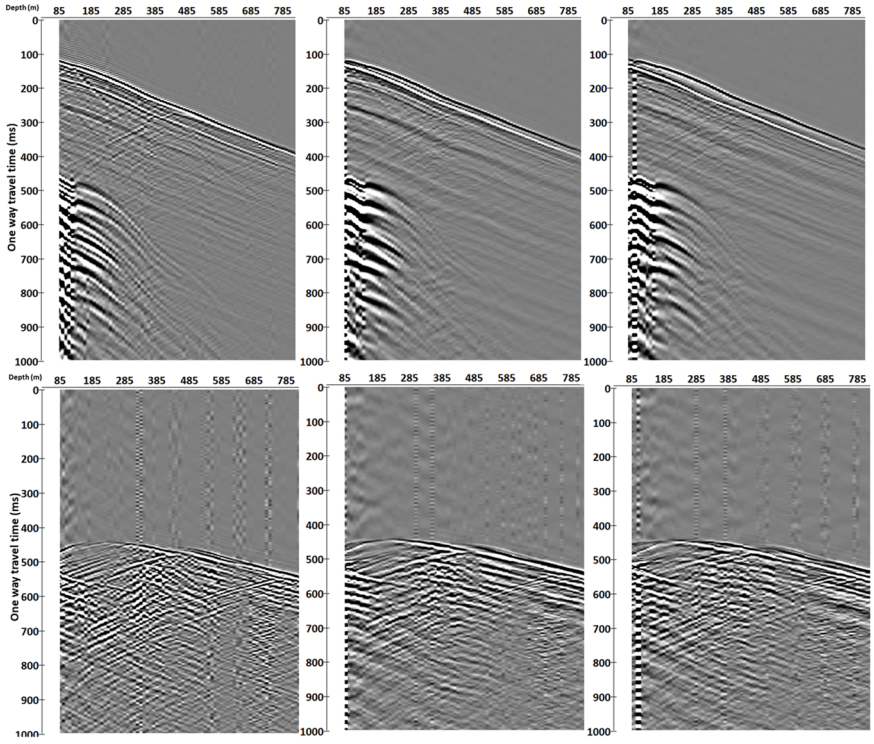

Figure 8. Gauge length simulation of 10 m (**left**), 50 m (**middle**) and 90 m (**right**), for near (**top**) and far (**bottom**) offset converted geophone.

5. Discussion

Our analysis shows that the conversion of geophone data (vertical particle velocity) to vertical strain rate brings the phase of the direct wave closer to the phase of DAS data (Figures 4 and 5). The polarity of the reflected waves in the converted geophone dataset also matches the DAS data. The amplitude response of the studied borehole geophones and DAS is similar after converting both datasets to strain rates (Figures 6 and 7). This is a surprising result considering that different factors affect geophones and DAS measurements. For example, the geophone amplitudes are affected by the type of a geophone and its performance, the probe's housing and the quality of the probe's coupling to the formation or the casing. The DAS amplitudes are affected by the designs of a cable and an interrogator, the cable's coupling with the formation and selected optical parameters. Nonetheless, the

amplitude spectra of the two datasets show similar absolute values (Figure 6), and the variations of the first-break amplitudes with depth are similar as well (Figure 7).

Apart from the higher noise level on geophone data observed for far offset, DAS and converted geophone records look similar. However, near-offset data with higher frequencies present in the record show a significant discrepancy in the phase of the direct arrivals (arrows in Figure 4). The discrepancy is better observed at shear waves, which could be caused by how the fibre reacts to S-waves. While we can assume that the effect linked to the gauge length dominates for relatively low frequencies, high frequencies may require pulse length effect also being taken into account.

For the same source effort (single shot), DAS and converted geophone amplitudes are similar for near offset. However, for far offset, the high-frequency part of the DAS spectrum (>100 Hz) looks constant even beyond the frequency of the sweep (150 Hz), which might indicate that this part of the spectrum is mostly noise (Figure 6). This agrees with earlier findings that the geophone has higher sensitivity with increased offset than DAS.

Similar strain-rate response between DAS and converted geophone datasets suggests using dense geophone data to simulate DAS measurements. Simulation of DAS response allows analysis of strain-rate wavefields and further understanding of DAS data (e.g., adaptation of existing particle velocity processing workflows to DAS workflows). For example, the gauge length is one of the most important parameters for DAS survey [13] as it affects not only the signal-to-noise ratio but also the wavefield distortion. Changing the gauge length can Introduce a ghost wave if the gauge length is not optimal for the recorded wavelength (Figure 8). In addition to this, we can observe the notches in k-spectrum, which are caused by the gauge length effect (Figure 9). In the absence of standardisation of DAS systems (i.e., different DAS systems may have fixed or variable gauge length parametrisation), one can study the gauge length effect from the converted geophone wavefield and potentially use it for the sensitivity optimisation for a target wavelength. Having data with densely spaced geophones allows one to simulate and study the effect of various gauge lengths by differentiating it on different bases.

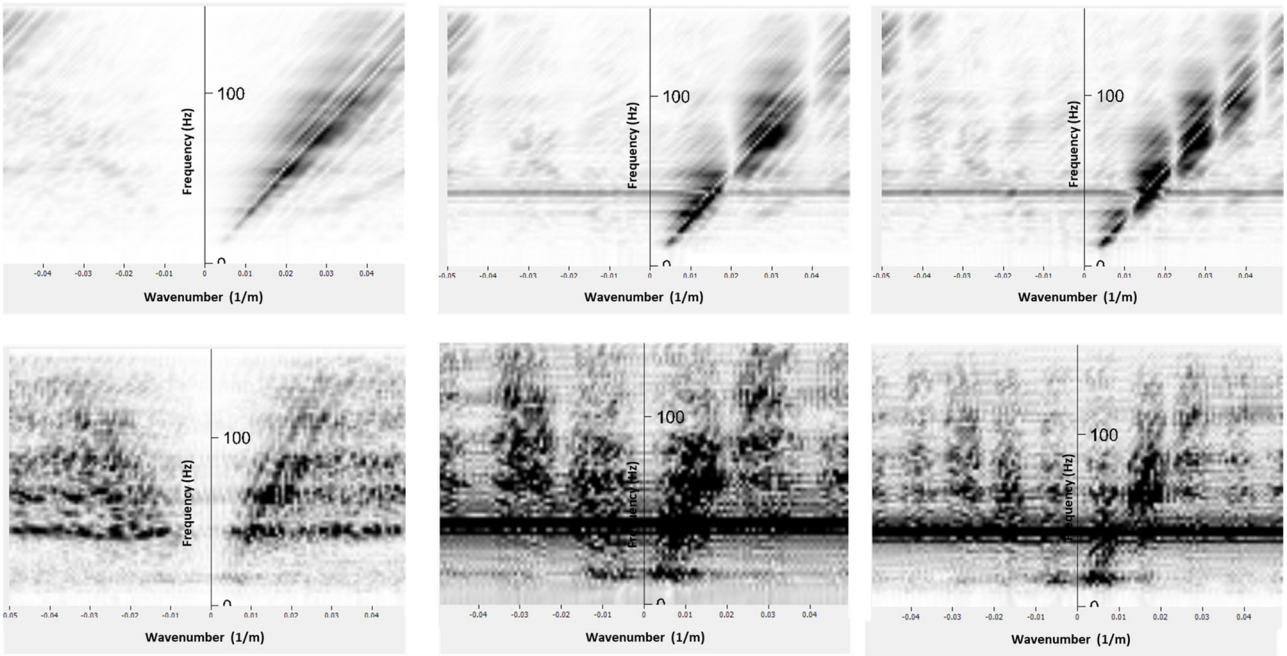

Figure 9. F-K spectrum for the converted geophone data with a simulated gauge length of 10 m (**left**), 50 m (**middle**) and 90 m (**right**) for near (**top**) and far (**bottom**) offset.

For purposes of comparing the same physical property collected with a different type of sensor, the conversion approach by differentiation of particle velocity over the gauge

length could be better than the integration of strain proposed by Bona, et al. [15] because the division with zero (for certain values of k) is avoided.

The first-break strain-rate amplitudes are calculated from the vibroseis data correlated with a pilot sweep. This process affects the phase of a signal. The vibrator output is defined in terms of its baseplate motion (e.g., displacement, velocity or acceleration). When correlation with a pilot sweep is performed on motion data, the resulting correlogram is assumed to be zero-phase [31]. Therefore, correlating strain data with a pilot sweep (representation of motion) may impact a phase of correlated DAS data. In addition to this, the effects of DAS parameters (pulse and gauge length) are shown to have a considerable effect on phase [15]. This needs to be studied further and considered when interpreting the DAS data.

6. Conclusions

We brought geophone and DAS measurements to the same property and calibrated them to the absolute strain rate. We compared the amplitude spectrum of the entire absolute strain-rate wavefield (uncorrelated) and the first-break amplitudes (correlated) for DAS and converted geophone. In addition to amplitude spectrum analysis, we simulated the DAS response with two additional gauge lengths.

We observed that DAS and geophone have similar absolute values of strain-rate amplitudes, despite different factors affecting the performance. The losses of seismic energy due to the geophone coupling and housing are similar to the losses in fibre-optic cable construction and installation. Albeit similarity in absolute response is surprisingly good, we do not expect this finding will be universal, different cable design, coupling, etc., can produce situations where geophone and DAS response can be different.

A denser geophone dataset can be used to simulate DAS response.

GeoLab provided an excellent opportunity for such kind of research. Different equipment can be tested and assessed versus the reference dataset. Data is publicly available.

Author Contributions: Conceptualisation, S.Z., R.P. and A.B.; methodology, S.Z., R.P., A.B. and K.T.; software, S.Z., R.P., E.S. and A.Y.; validation, S.Z., K.T. and R.P.; formal analysis, S.Z., A.B. and R.P.; investigation, R.P., K.T., A.B., E.S. and A.Y.; data curation, R.P., S.Z. and A.Y.; writing—original draft preparation, S.Z.; writing—review and editing, K.T., A.Y. and R.P.; visualisation, S.Z. and A.B.; supervision, R.P., A.B. and K.T.; project administration, R.P. and S.Z. All authors have read and agreed to the published version of the manuscript.

Funding: The work has been supported by the Mineral Exploration Cooperative Research Centre whose activities are funded by the Australian Government's Cooperative Research Centre Program (2022/9). Part of this work has been supported by Curtin University Faculty of Science and Engineering Research and Development Committee Small Grants 2020 and Curtin Reservoir Geophysical Consortium.

Institutional Review Board Statement: Not applicable.

Informed Consent Statement: Not applicable.

Data Availability Statement: The baseline geophone dataset and corresponding DAS dataset are available at Research Data Australia (https://doi.org/10.25917/7h0e-d392).

Acknowledgments: The authors are grateful to colleagues Stanislav Glubokovskikh, Roman Isaenkov, Dominic Howman and Murray Hehir for their technical support during the field experiment. The authors are also grateful to Silixa Ltd. for proving access to DAS equipment and advice.

Conflicts of Interest: The authors declare no conflict of interest.

References

1. Evenden, B.S.; Stone, D.R. Instrument Performance and Testing. Lubrecht & Cramer, Limited: New York, NY, USA, 1971; Volume 2.
2. Parker, T.; Gillies, A.; Shatalin, S.; Farhadiroushan, M. The intelligent distributed acoustic sensing. *Proc. SPIE Int. Soc. Opt. Eng.* **2014**, *9157*, 525–528. [CrossRef]
3. Galperin, E.I.; White, J.E. *Vertical Seismic Profiling*; Society of Exploration Geophysicists: Tulsa, Okla, 1974.

4. Hardage, B.A. *Vertical Seismic Profiling*; Geophysical Press: London, UK; Worldwide Distributors, Expro Science Publications: Amsterdam, The Netherlands, 1983.
5. Mateeva, A.; Lopez, J.; Potters, H.; Mestayer, J.; Cox, B.; Kiyashchenko, D.; Wills, P.; Grandi, S.; Hornman, K.; Kuvshinov, B.; et al. Distributed acoustic sensing for reservoir monitoring with vertical seismic profiling. *Geophys. Prospect.* **2014**, *62*, 679–692. [CrossRef]
6. Correa, J.; Egorov, A.; Tertyshnikov, K.; Bona, A.; Pevzner, R.; Dean, T.; Freifeld, B.; Marshall, S. Analysis of signal to noise and directivity characteristics of DAS VSP at near and far offsets—A CO2CRC Otway Project data example. *Lead. Edge* **2017**, *36*, a991–a994. [CrossRef]
7. Sidenko, E.; Pevzner, R.; Bona, A.; Tertyshnikov, K. Experimental Comparison of Directivity Patterns of Straight and Helically Wound DAS Cables. In Proceedings of the 82nd EAGE Annual Conference & Exhibition, Amsterdam, The Netherlands, 18–21 October 2021; pp. 1–5.
8. Wang, H.F.; Zeng, X.; Miller, D.E.; Fratta, D.; Feigl, K.L.; Thurber, C.H.; Mellors, R.J. Ground motion response to an ML 4.3 earthquake using co-located distributed acoustic sensing and seismometer arrays. *Geophys. J. Int.* **2018**, *213*, 2020–2036. [CrossRef]
9. Mestayer, J.; Cox, B.; Wills, P.; Kiyashchenko, D.; Lopez, J.; Costello, M.; Bourne, S.; Ugueto, G.; Lupton, R.; Solano, G.; et al. Field trials of distributed acoustic sensing for geophysical monitoring. In *SEG Technical Program Expanded Abstracts 2011*; Society of Exploration Geophysicists: Houston, TX, USA, 2011; pp. 4253–4257.
10. Barberan, C.; Allanic, C.; Avila, D.; Hy-Billiot, J.; Hartog, A.; Frignet, B.; Lees, G. Multi-offset Seismic Acquisition Using Optical Fiber Behind Tubing. In Proceedings of the 74th EAGE Conference and Exhibition Incorporating EUROPEC 2012, Copenhagen, Denmark, 4–7 June 2012. [CrossRef]
11. Mateeva, A.; Mestayer, J.; Cox, B.; Kiyashchenko, D.; Wills, P.; Lopez, J.; Grandi, S.; Hornman, K.; Lumens, P.; Franzen, A.; et al. Advances in Distributed Acoustic Sensing (DAS) for VSP. In *SEG Technical Program Expanded Abstracts 2012*; Society of Exploration Geophysicists: Houston, TX, USA, 2012; pp. 1–5.
12. Daley, T.; Freifeld, B.; Ajo-Franklin, J.; Dou, S.; Pevzner, R.; Shulakova, V.; Kashikar, S.; Miller, D.; Goetz, J.; Henninges, J.; et al. Field testing of fiber-optic distributed acoustic sensing (DAS) for subsurface seismic monitoring. *Lead. Edge* **2013**, *32*, 699–706. [CrossRef]
13. Dean, T.; Cuny, T.; Hartog, A.H. The effect of gauge length on axially incident P-waves measured using fibre optic distributed vibration sensing. *Geophys. Prospect.* **2017**, *65*, 184–193. [CrossRef]
14. Daley, T.M.; Miller, D.E.; Dodds, K.; Cook, P.; Freifeld, B.M. Field testing of modular borehole monitoring with simultaneous distributed acoustic sensing and geophone vertical seismic profiles at Citronelle, Alabama. *Geophys. Prospect.* **2016**, *64*, 1318–1334. [CrossRef]
15. Bona, A.; Dean, T.; Correa, J.; Pevzner, R.; Tertyshnikov, K.V.; Van Zaanen, L. Amplitude and Phase Response of DAS Receivers. In Proceedings of the 79th EAGE Conference and Exhibition 2017, Paris, France, 12–15 June 2017; Volume 2017, pp. 1–5. [CrossRef]
16. Isaenkov, R.; Glubokovskikh, S.; Tertyshnikov, K.; Pevzner, R.; Bona, A. Effect of Rocks Stiffness on Observed DAS VSP Amplitudes. In Proceedings of the EAGE Workshop on Fiber Optic Sensing for Energy Applications in Asia Pacific, Kuala Lumpur, Malaysia, 9–11 November 2020; pp. 1–5.
17. Pevzner, R.; Bona, A.; Correa, J.; Tertyshnikov, K.; Palmer, G.; Valishin, O. Optimising DAS VSP data acquisition parameters: Theory and experiments at Curtin training well facility. In Proceedings of the 80th EAGE Conference and Exhibition 2018, Copenhagen, Denmark, 11–14 June 2018; p. WS08.
18. Sidenko, E.; Bona, A.; Pevzner, R.; Issa, N.; Tertyshnikov, K. Influence of Interrogators' Design on DAS Directional Sensitivity. In Proceedings of the EAGE Workshop on Fiber Optic Sensing for Energy Applications in Asia Pacific, Kuala Lumpur, Malaysia, 9–11 November 2020; pp. 1–5.
19. Lawton, D.C.; Osadetz, K.G.; Saeedfar, A. CCS Monitoring Technology Innovation at the CaMI Field Research Station, Alberta, Canada. In Proceedings of the EAGE/SEG Research Workshop 2017, Trondheim, Norway, 28–31 August 2017. [CrossRef]
20. Correa, J.; Freifeld, B.; Robertson, M.; Pevzner, R.; Bona, A.; Popik, D.; Tertyshnikov, K.; Daley, T. 3D Vertical Seismic Profiling Acquired Using Fibre-Optic Sensing Das—Results From The CO2CRC Otway Project. *ASEG Ext. Abstr.* **2018**, *2018*, 1–5. [CrossRef]
21. Tertyshnikov, K.; Pevzner, R.; Freifeld, B.; Ricard, L.; Avijegon, A. DAS VSP for Characterisation and Monitoring of the CO_2 Shallow Release Site: CSIRO In-Situ Laboratory Case Study. In Proceedings of the Fifth EAGE Workshop on Borehole Geophysics, The Hauge, The Netherlands, 18 November 2019; pp. 1–5.
22. Sun, Y.; Xue, Z.; Hashimoto, T.; Lei, X.; Zhang, Y. Distributed Fiber Optic Sensing System for Well-Based Monitoring Water Injection Tests—A Geomechanical Responses Perspective. *Water Resour. Res.* **2020**, *56*, e2019WR024794. [CrossRef]
23. Lindsey, N.J.; Martin, E.R.; Dreger, D.S.; Freifeld, B.; Cole, S.; James, S.R.; Biondi, B.L.; Ajo-Franklin, J.B. Fiber-Optic Network Observations of Earthquake Wavefields. *Geophys. Res. Lett.* **2017**, *44*, 11792–11799. [CrossRef]
24. Lindsey, N.J.; Dawe, T.C.; Ajo-Franklin, J.B. Illuminating seafloor faults and ocean dynamics with dark fiber distributed acoustic sensing. *Science* **2019**, *366*, 1103–1107. [CrossRef] [PubMed]
25. Ajo-Franklin, J.B.; Dou, S.; Lindsey, N.J.; Monga, I.; Tracy, C.; Robertson, M.; Rodriguez Tribaldos, V.; Ulrich, C.; Freifeld, B.; Daley, T.; et al. Distributed Acoustic Sensing Using Dark Fiber for Near-Surface Characterization and Broadband Seismic Event Detection. *Sci. Rep.* **2019**, *9*, 1328. [CrossRef] [PubMed]

26. Aldawood, A.; Alfataierge, E.; Bakulin, A. Introducing a New DAS Test Facility for Evaluating Emerging DAS Technologies. In Proceedings of the First EAGE Workshop on Fibre Optic Sensing, Amsterdam, The Netherlands, 9–11 March 2020; Volume 2020, pp. 1–5. [CrossRef]
27. Wuestefeld, A.; Stokkan, S.; Baird, A.; Oye, V. NOR-FROST: A near-surface test site for fibre optic sensing. In Proceedings of the EAGE GeoTech 2021 Second EAGE Workshop on Distributed Fibre Optic Sensing, Online, 1–2 March 2021; Volume 2021, pp. 1–4. [CrossRef]
28. Correa, J.; Dean, T.; Van Zaanen, L.; Tertyshnikov, K.; Pevzner, R.; Bona, A. A Comparison of DAS and Geophones for VSP Acquisition At a Dedicated Field Laboratory. In Proceedings of the 79th EAGE Conference & Exhibition 2017, Paris, France, 12–15 June 2017; pp. 1–5.
29. Shulakova, V.; Tertyshnikov, K.; Pevzner, R.; Kovalyshen, Y.; Gurevich, B. Ambient seismic noise in an urban environment: Case study using downhole distributed acoustic sensors at the Curtin University campus in Perth, Western Australia. *Explor. Geophys.* **2022**, *53*, 620–633. [CrossRef]
30. Bakku, S.K. Fracture Characterization from Seismic Measurements in a Borehole. Ph.D. Thesis, Massachusetts Institute of Technology, Cambridge, MA, USA, 2015.
31. Sallas, J.J. Seismic vibrator control and the downgoing P-wave. *Geophysics* **1984**, *49*, 732–740. [CrossRef]